



Feasibility study and material selection for powder-bed fusion process in printing of denture clasps

Kenan Ma^{a,1}, Hu Chen^{a,1}, Yanru Shen^a, Yuqing Guo^a, Weiwei Li^a, Yong Wang^a,
Yicha Zhang^{b,**}, Yuchun Sun^{a,*}

^a Center of Digital Dentistry, Faculty of Prosthodontics, Peking University School and Hospital of Stomatology & National Center for Stomatology & National Clinical Research Center for Oral Diseases & National Engineering Research Center of Oral Biomaterials and Digital Medical Devices & Beijing Key Laboratory of Digital Stomatology & Research Center of Engineering and Technology for Computerized Dentistry Ministry of Health & NMPA Key Laboratory for Dental Materials, No.22, Zhongguancun South Avenue, Haidian District, Beijing, 100081, PR China

^b Mechanical Engineering and Design Department, Université de Bourgogne Franche-Comté, Université de Technologie de Belfort-Montbéliard, ICB UMR CNRS 6303, 90010, Belfort Cedex, France

ARTICLE INFO

Keywords:

Selective laser melting
Process optimization
Circumferential clasp
Retention
Dental prosthesis
Undercut

ABSTRACT

Background and objective: The retention of selective laser melting (SLM)-built denture clasps is inferior to that of cast cobalt-chromium (Co-Cr) clasps engaging 0.01-in undercuts, which are commonly used in clinical practice. Either the clasps engage in excessively deep undercuts or inappropriate printing process parameters are applied. With appropriate undercut engagement and levels of process parameters, the retention of SLM-built clasps (including Co-Cr, commercially pure titanium [CP Ti], and Ti alloy [Ti-6Al-4V] ones) may be comparable to that of cast Co-Cr clasps. Therefore, this feasibility study aimed to evaluate their retention to guide dentists during material selection for the powder-bed fusion process during the printing of denture clasps.

Methods: We engaged the clasp arm at an appropriate undercut depth (0.01 or 0.02 in), built clasps at the orientation of their longitudinal axes approximately parallel to the build platform, generated square prism support structures at a critical overhang angle of 30°, applied optimized laser parameters (laser power, scan speed, and hatch space), and adopted annealing treatment for Co-Cr, CP Ti, and Ti-6Al-4V clasps. After post-processing and accuracy measurement, an insertion/removal test of the clasps for 15,000 cycles was performed to simulate 10 years of clinical use, and the retentive force was recorded every 1500 cycles. Permanent deformation of the retentive arms of the clasps was measured. Cast Co-Cr clasps engaging 0.01-in undercuts were designated the control group.

Results: The initial retentive forces of the SLM-built Co-Cr clasps engaging 0.01-in undercuts and CP Ti and Ti-6Al-4V clasps engaging 0.02-in undercuts were comparable to those of the control group. SLM-built Co-Cr clasps engaging 0.01-in undercuts and Ti-6Al-4V clasps engaging 0.02-in undercuts had similar final retentive force and less permanent deformation compared with those of the control group; SLM-built CP Ti clasps engaging 0.02-in undercuts had lower final retentive force and greater permanent deformation.

Conclusions: Considering the long-term retention and permanent deformation of the retentive arms, Co-Cr and Ti-6Al-4V alloys, except CP Ti, are recommended for printing denture clasps. SLM-built Co-Cr clasps should engage 0.01-in undercuts, and Ti-6Al-4V clasps should engage 0.02-in undercuts.

1. Introduction

World Health Organization (WHO) estimated that by 2030, 1.4 billion individuals worldwide would be aged 60 years or above [1].

Tooth loss is highly prevalent among older adults [2–4]. Some national oral health survey reports show that the average number of missing teeth of older adults is 5.5 in China [2], 7.3 in the United States [5], 11.1 in Germany [3], and 8.8 in Australia [4]. The prevalence of edentulism

* Corresponding author.

** Corresponding author.

E-mail addresses: yicha.zhang@utbm.fr (Y. Zhang), kqsyrc@bjmu.edu.cn (Y. Sun).

¹ Equal contribution of both first authors.

(total tooth loss) is much lower than that of partial edentulism among older adults [2–4]. Missing teeth of partially edentate adults can be restored with dental implant restorations, fixed partial dentures, or removable partial dentures (RPDs), of which RPDs are in greatest demand owing to a wide range of indications and relative affordability. A conventional RPD comprises a metal framework fabricated by traditional investment casting and a resin base fabricated by flasking and packing. The fabrication of conventional RPDs is time-consuming, and casting defects often occur, particularly when casting pure titanium and titanium alloys. Over the past 20 years, computer-aided design/computer-aided manufacturing (CAD/CAM) technology has been gradually applied to the fabrication of RPDs. Recently, a few researchers have attempted to manufacture a metal framework and resin base using CAD/CAM and to assemble them into an RPD [6,7]. However, the digitalization of RPDs mainly involves the fabrication of a metal framework because the CAM technology for the resin base is still developing. Selective laser melting (SLM) is replacing conventional investment casting and is becoming routine in removable prosthodontics. SLM powder metal materials used to manufacture RPD frameworks include cobalt-chromium (Co–Cr) alloys, titanium alloys (Ti–6Al–4V), and commercially pure titanium (CP Ti) [8]. SLM technology has the advantages of high production efficiency and low cost, and the relative density of SLM-built metal parts can be as high as 99.9% [9–11]. SLM-built RPD frameworks are widely used in clinical practice.

The accuracy and adaption of SLM-built RPD frameworks are similar to those of cast ones [12–15]. Their long-term retention must also meet clinical requirements to allow SLM-built RPDs to function stably in the patients' mouths for a long time. The retention of circumferential clasps, the most common retainers of RPDs, has attracted the attention of many researchers and dentists. Clasp retention can be achieved by two main methods: 1) Simplifying the clasp as a cantilever beam with the same cross-sectional shape. A load is applied on the free end of the cantilever beam to make a vertical deflection of 0.01 or 0.02 in (0.25 or 0.50 mm), simulating the clasp arm engaging in 0.01-in or 0.02-in undercuts. The load indirectly deflects the retention performance of the clasp [16,17]. 2) A more direct approach would be to insert a clasp on the tooth die and then dislodge it. The maximum vertical component of the force of the tooth die on the clasp is considered to be the retentive force of the clasp [18,19]. Typically, researchers insert or dislodge the clasp for 10,000 or 15,000 cycles to simulate the conditions experienced by an RPD placed intraorally for several years, assuming that patients would perform four complete cycles per day. The retentive force of SLM-built clasps should neither be too small to ensure good intraoral retention of the RPD nor too large for patients to remove their dentures safely. Cast Co–Cr frameworks are most commonly used in clinical practice. The retention of clasps made of other metals is commonly evaluated by comparing their retentive force with that of the cast Co–Cr clasps.

The long-term retention performance of SLM-built metal clasps is better than that of cast-metal clasps. Kim et al. [17] showed that when the vertical deflection was 0.01 inches, the bending load of annealed SLM specimens was 3.12 ± 0.44 N, which was significantly higher than that of unannealed SLM specimens (2.25 ± 0.99 N) but lower than that of cast specimens (8.87 ± 1.24 N). This indicates that annealing treatment can improve the elastic modulus of metals and thus improve the retention performance of metal clasps. The SLM-built Co–Cr clasps are more flexible and less rigid than cast Co–Cr clasps [17]. However, the printing process has not been comprehensive [17]. In the study by Kajima et al. [20], when the deflection was 0.01 inches, SLM-built Co–Cr clasps built with the longitudinal axes inclined by 0° , 45° , and 90° had slightly lower bending loads than cast Co–Cr clasps (9.6 ± 0.5 N). After 10^6 cycles of loading/unloading, clasp specimens built at angles of 45° and 90° fractured, and clasp specimens built at an angle of 0° had slightly lower bending loads than those of cast Co–Cr clasps (9.3 ± 0.3 N). During SLM printing, the laser spot moves rapidly, rapid solidification occurs in the molten pool, and a smaller grain size is formed. This leads to a higher yield and tensile strength of the SLM-built Co–Cr alloy

than that of the cast Co–Cr alloy [20,21]. However, the SLM-built specimens exhibited a lower fatigue strength and life than the cast specimens. This may be related to the molten pool boundaries. Wen et al. [22] reported that the fracture of SLM-built parts initiated at the molten pool boundaries, and cracks extended along the boundaries in a tensile fracture. The fracture surfaces of the clasp specimens built at an angle of 90° were approximately parallel to the molten-pool boundaries. For comparison, the fracture surfaces of the clasp specimens built at an angle of 0° were perpendicular to the molten pool boundaries. Cracks can easily propagate along molten-pool boundaries. In addition to the build orientation, the support structures help improve the fatigue performance and, thus, the long-term retention performance of the clasps. The support structures reduced the residual strain during the SLM process and helped to prevent micro-cracks caused by thermal distortion. Moreover, the supported specimens cooled more rapidly and formed finer grains than the unsupported specimens [23]. In another study [23], when the deflection was 0.02 inches, the fatigue life of supported Co–Cr clasp specimens was twice as long as that of unsupported ones. Laser parameters such as laser power, scan speed, and hatch space also undoubtedly affect the mechanical properties and microstructure of SLM-built parts [11] and thus, affect the retention performance of metal clasps. However, few studies have investigated these factors in detail. In addition to the retention of SLM-built Co–Cr clasps, some researchers have reported that the retention of SLM-built Ti–6Al–4V clasps hardly meets the clinical requirements. Tan et al. [24] showed that all specimens of SLM-built Ti–6Al–4V clasps fractured after 4000 cycles of insertion/removal. The fracture of clasps was attributed to their engagement in excessive undercuts (0.03 in), which led to the load on the clasps exceeding their fatigue strength. This suggests that SLM-built cast alloy clasps should engage less than 0.03-in undercuts.

We can adjust the build orientation; generate appropriate support structures; set proper levels of laser parameters (such as laser power, scan speed, and hatch space); and perform annealing treatment to improve the tensile and fatigue properties of SLM-built parts, or consider the design of clasps, such as engaging the clasp arm at appropriate undercut depths to ensure the retention performance of SLM-built metal clasps. The retention of SLM-built metal clasps is purportedly comparable to that of cast Co–Cr clasps, which are currently commonly used in clinical practice. Therefore, this feasibility study aimed to evaluate the long-term retention of 3D-printed clasps (including Co–Cr, CP Ti, and Ti–6Al–4V) to guide dentists in material selection for the powder-bed fusion process during the printing of denture clasps.

2. Materials and methods

2.1. Design of the tooth die and clasps

The maxillary left first premolar of the resin cast was prepared for the distal rest seat and guiding plane (Fig. 1a). The rest seat was a rounded triangular shape with its apex nearest to the center of the premolar. The base of the triangular shape was approximately one-half the buccolingual width of the premolar. The marginal ridge was lowered to allow the thickness of the rest to be approximately 1.5 mm. The guiding plane was approximately two-thirds of the occluso-gingival height of the distal surface of the premolar [25]. The prepared abutment tooth was sprayed using a 3D scan spray (YIQIAO SCAN, Dalian Yiqiao Medical Devices Co. Ltd., China) and scanned using a 3D scanner (D2000, 3Shape A/S, Denmark). Digital scans of the prepared abutment tooth were sculpted to ensure undercuts on the buccal surface of the abutment tooth; however, no undercuts were made on the lingual surface using reverse engineering software (Geomagic Studio 2014, 3D Systems, US). A cylindrical base was virtually added to the bottom of the abutment tooth using preparation software (Magics 21.0, Materialise, Belgium) to fix the tooth die in the chewing simulator (CS4.2, SD Mechatronik, Germany) (Fig. 1b). In routine clinical practice, RPD clasps engaging 0.01 or 0.02-in undercuts were designed on the tooth die (Fig. 2a–d)

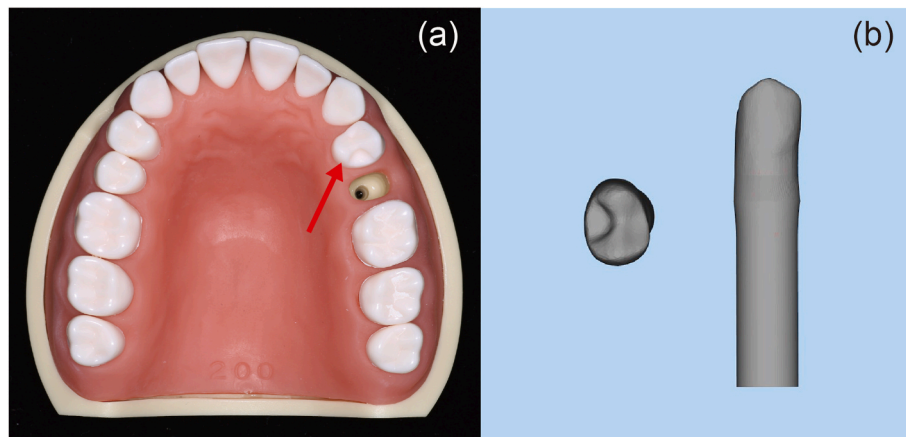


Fig. 1. Design of tooth die. (a) Prepared first premolar. (b) Computer-aided design (CAD) data of tooth die.

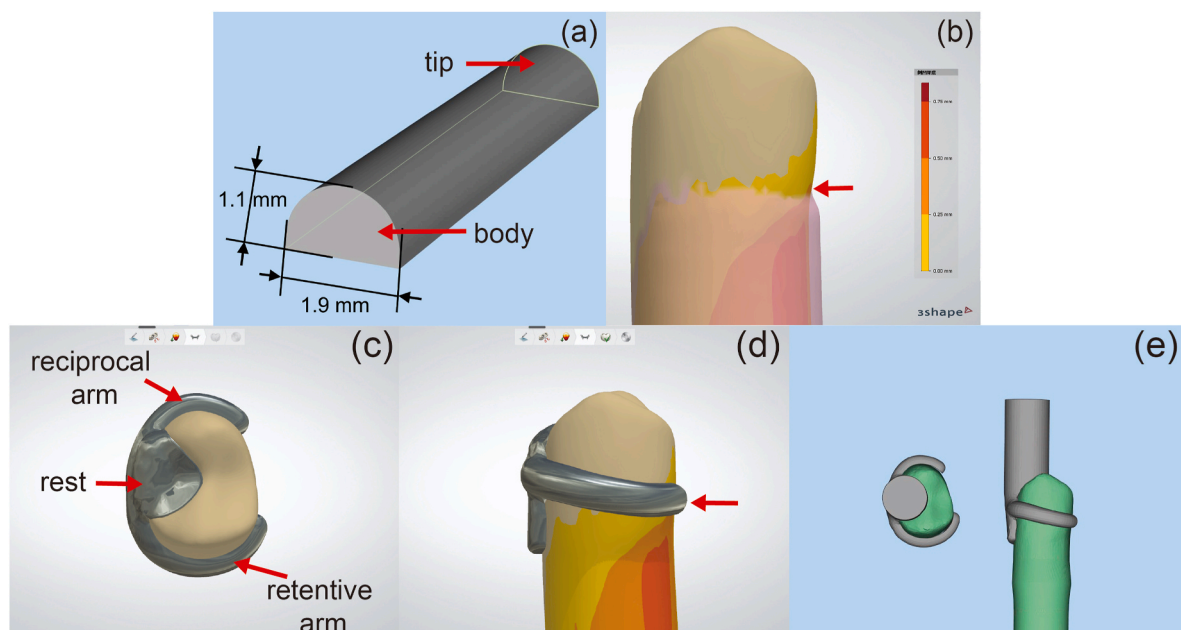


Fig. 2. Design of clasps. (a) Profile of clasp arm. (b) Undercut. (c) Retentive arm, reciprocal arm, and rest of clasp. (d) Retentive arm tip engages undercut. (e) Clasp specimen.

using dental CAD software (Dental System 2019 Premium, 3Shape A/S, Denmark). The size of the clasp arm (1.9-mm width/1.1-mm thickness at the body, 0.8-taper ratio from the tip to the body) and thickness of the proximal plate (0.8 mm) are the default values provided by the CAD software vendor. A cylindrical bar was virtually added to the top of the rest using the Geomagic Studio 2014 software to fix the clasps in the chewing simulator (Fig. 2e).

2.2. Experimental design

The metal powders used in dentistry include Co–Cr alloys, CP Ti, and Ti–6Al–4V [8]. The retention of these three types of metal clasps was evaluated by comparing them with those of cast Co–Cr clasps engaging 0.01-in undercuts, the most commonly used clasps in clinical practice. The retentive force of the clasp is derived from the friction force between the clasp and tooth and adhesion force owing to the surface tension of the clasp-saliva-tooth system. The adhesion force was assumed to be 1 N, which is significantly less than the friction force [26]. The elastic modulus determines the friction between the clasp and tooth. Previous studies have shown that the elastic modulus of SLM-built Co–Cr is

comparable to that of cast Co–Cr alloys, while the elastic modulus of CP Ti and Ti–6Al–4V is nearly half that of Co–Cr alloys [8,19,27]. It could be predicted that the retention of the SLM-built CP Ti and Ti–6Al–4V clasps was not as good as that of the control group. Common clinical practice is to make clasps engage in deeper undercuts, for instance, 0.02-in undercuts. In the study by Yager et al. [16], SLM-built Co–Cr cantilever beams were permanently deformed when the vertical deflection at their tip was 0.02 inches. SLM-built Ti–6Al–4V clasps could engage 0.02-in undercuts in the study by Xie et al. [19]; however, they could not engage 0.03-in undercuts in the study by Tan et al. [24]. Tan et al. [24] observed that all SLM-built Ti–6Al–4V clasp specimens fractured after 4000 insertion/removal cycles. Therefore, only 0.01 and 0.02-in undercuts were used in this study. As shown in Table 1, Co–Cr, CP Ti, and Ti–6Al–4V clasps with 0.01 or 0.02-in undercut engagement were printed, and each group had six specimens.

2.3. Manufacturing of clasps and tooth dies

Table 2 lists the main chemical components of the cast Co–Cr alloy and the characteristics of SLM metal powders used in this study. Inspired

Table 1

Experimental design. Co–Cr, Cobalt-chromium. CP Ti, Commercially pure titanium. Ti alloy, Ti–6Al–4V.

ID	Group	N	Metal type	Undercut engagement (in)
0	Control	6	Cast Co–Cr	0.01
1	Experimental	6	Co–Cr	0.01
2	Experimental	6	Co–Cr	0.02
3	Experimental	6	CP Ti	0.01
4	Experimental	6	CP Ti	0.02
5	Experimental	6	Ti–6Al–4V	0.01
6	Experimental	6	Ti–6Al–4V	0.02

Table 2

Main characteristics of selective laser melting metal powders. NA, Not available. Co–Cr, Cobalt-chromium. CP Ti, Commercially pure titanium. Ti alloy, Ti–6Al–4V.

Metal	Cast Co–Cr	Co–Cr powder	CP Ti powder	Ti–6Al–4V powder
Manufacturer	BEGO GmbH	DPR Materials Co. Ltd.	Weilali Materials Co. Ltd.	Shangcai 3D Technology Co. Ltd.
Chemical composition (weight%)	Co, 63.0% Cr, 30.0% Mo, 5.0%	Co, (62–66)% Cr, (23–27)% Mo, (4–6)% W, (4–6)%	Ti ≥ 99.71%	Al, (5.50–6.75)% V, (3.50–4.50)%
Particle size (µm)	–	10–45	15–53	0–45
D10 (µm)	–	15	20.7	≤15
D50 (µm)	–	28	35.3	30–40
D90 (µm)	–	44	56.5	≤63
Apparent density (g/cm ³)	–	≥4	2.36	NA
Tapped density (g/cm ³)	–	≥4.5	NA	NA
Flowability (s/50 g)	–	≤40	37.54	<40

by the study of Kajima et al. [20], we built clasps in the orientation of the cylindrical bar at the bottom and clasp arms at the top. The critical overhang angle was 30°, and square prism support structures were generated automatically using slicer software (P3DS, Profeta Co. Ltd., China) (Fig. 3). The layer thickness was 0.03 mm for all specimens as usual [9]. Co–Cr clasp specimens were printed using an SLM printer (Tr150, Profeta Co. Ltd., China) under a protective atmosphere of nitrogen. CP Ti and Ti–6Al–4V clasp specimens were printed using another SLM printer (Ti150, Profeta Co. Ltd., China) under argon. The diameter of the laser beam was 0.065 mm. Infill hatch lines were scanned using the zigzag strategy. This strategy is the most commonly used one for printing geometries with complex freeform surfaces [28]. Then the laser beam contoured the layer along its perimeter twice with spot

compensation when scanning the outer contour set to 0.07 mm. The rotation angle of the scanning patterns between the layers was set to 67° [29]. The volumetric energy density $E=P/(v*h*t)$, where P is laser power, v is scan speed, h is hatch space, and t is layer thickness, directly affecting the density and porosity of build parts [30]. The mechanical properties of build parts are closely related to their density and porosity. Inspired by previous studies [9,11,31,32], the proper levels of laser power, scan speed, and hatch space in the printing of Co–Cr, CP Ti, and Ti–6Al–4V powders were set. Table 3 lists the main process parameters. Castable resin patterns of the clasp with 0.01-in undercut engagement were printed using a digital light-processing printer (Lite600HD, UnionTech Co. Ltd., China) and then invested and cast into Co–Cr (Wironit extra-hard, BEGO GmbH, Germany) clasp specimens, which were the control group. The CAD data of the tooth die were sent to a dental laboratory (Beijing Liaison Dental Technology Co., Ltd), and ASTM 304 stainless steel dies were milled using a milling machine (408 MT, Willemin-Macodel SA, Switzerland), according to the manufacturer’s instructions.

2.4. Postprocessing of clasps

The 3D-printed clasp specimens were annealed in a vacuum annealing furnace (RZF1200, Shanghai Refan Co. Ltd., China). They were heated to the annealing temperature of the metal at a rate of 15 °C/min, stabilized for 60 min, and cooled to the room temperature (23 °C) in the furnace. The annealing temperature was 1190 °C for the Co–Cr alloy, 650 °C for CP Ti, and 850 °C for Ti–6Al–4V. The 3D-printed clasp specimens were cut from building platforms using a wire-cutting machine (DK7728, Tianlong Numerical Controlled Co. Ltd., China). After manual removal of the support structures, they were sandblasted using 100-µm white fused alumina particles under a pressure of 0.4–0.6 MPa. They were then ground using tungsten carbide burs at a speed of 20,000–30,000 r/min to remove residual supports, nodules, and burrs, and polished using carborundum points at the same speed. The cast Co–Cr clasp specimens were sandblasted and polished similarly. Fig. 4 shows a clasp specimen and tooth die.

Table 3

Main process parameters for selective laser melting metallic powders. Co–Cr, Cobalt-chromium. CP Ti, Commercially pure titanium. Ti alloy, Ti–6Al–4V.

Process parameters	Co–Cr alloy	CP Ti	Ti–6Al–4V
Layer thickness (mm)	0.03	0.03	0.03
Scan strategy	Zigzag	Zigzag	Zigzag
Scan speed (mm/s)	800	1000	800
Laser power (W)	120	120	135
Hatch space (mm)	0.085	0.08	0.085

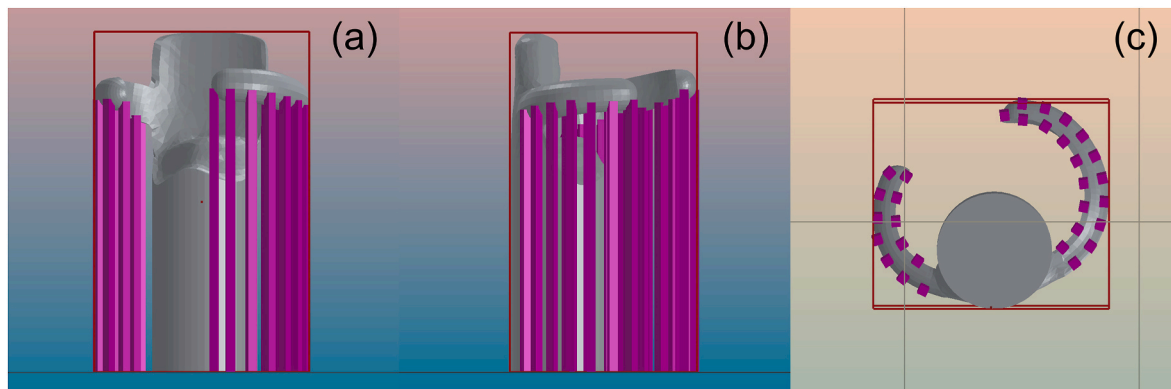


Fig. 3. Clasp specimen and support structures. (a) Back side view. (b) Right side view. (c) Bottom side view.



Fig. 4. Fabrication of tooth die and clasp.

2.5. Measurement of accuracy

The accuracy of clasps affects their retention. If a denture clasp has low accuracy, the denture cannot be seated well in the patient's mouth and will not have a good retention performance. Therefore, the accuracy of the clasp specimens was evaluated before their retention evaluation. There are two main indices for evaluating the accuracy of the clasps. One is adaption, that is, the gap between the intaglio surface of the clasp and tooth die after the clasp is seated on the tooth die. The second is the deviation of the scan data of the clasp from the original CAD data. The latter method was adopted in this study because it was easy to perform. Digital scans of all the clasp specimens were obtained using D2000. Before scanning, the specimens were sprayed using a 3D scan spray. The scan data (*Scan Data A*) of each clasp specimen were initially aligned with the CAD data through N-point alignment using Geomagic Studio 2014. Curves were drawn on the CAD data to select the clasp arms, rest, and proximal plate area, and then projected onto *Scan Data A*. The selected area of *Scan Data A* of each clasp specimen was aligned with that of the CAD data using best-fit alignment. The root mean square (RMS) representing the 3D deviation between the selected area of *Scan Data A* of each clasp specimen and that of the CAD data, named RMS_{acc} , was calculated (Fig. 5a). Similarly, the RMS between the scan data of each tooth die and the CAD data was calculated (Fig. 5b).

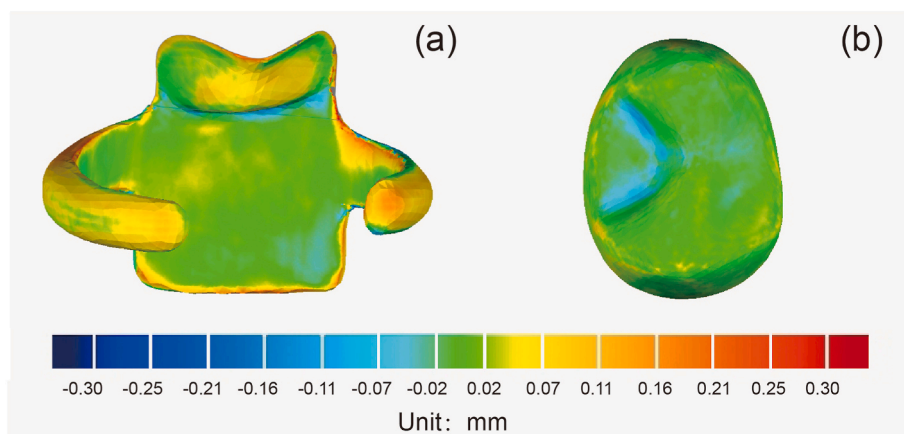


Fig. 5. Accuracy measurement of clasp and tooth die. (a) Clasp. (b) Tooth die.

2.6. Insertion/removal of clasps

Each clasp specimen was screwed for antagonist administration. The responding tooth die was embedded in the specimen holder with an auto-polymerizing acrylic resin (Technovit 4000, Kulzer, Germany) (Fig. 6a). A force sensor is placed in the specimen chamber. The test conditions were maintained at room temperature (23 °C) under wet conditions (with purified water). The clasp specimen moved down and up with a 15-mm amplitude and 60-mm/s speed (Fig. 6b). The maximum vertical force at which the clasp specimen was dislocated was regarded as the retentive force for each cycle [10–13,18,19]. The average retentive force during cycles 100–109 was named the initial retentive force, f_0 . The averages of the retentive force during the cycles 1500–1509, 3000–3009, 4500–4509, 6000–6009, 7500–7509, 9000–9005, 10,500–10509, 12,000–12009, 13,500–13509, and 15,000–15009 were measured and calculated as f_1 , f_2 , f_3 , f_4 , f_5 , f_6 , f_7 , f_8 , f_9 , and f_{10} , respectively. If a clasp specimen fractured, another specimen was added to the group in which it failed.

2.7. Permanent deformation of retentive arms

After the insertion/removal tests, digital scans of the unfractured clasp specimens were obtained using a scanner D2000. The scan data of each clasp specimen after the insertion/removal test were named *Scan Data B*. *Scan Data B* of each clasp specimen were aligned initially with its *Scan Data A* through N-point alignment using Geomagic Studio 2014. Curves were drawn on *Scan Data A* of each clasp specimen to select the reciprocal arm, rest, and proximal plate area and then projected onto its *Scan Data B*. The selected area of *Scan Data B* of each clasp specimen was aligned with that of its *Scan Data A* through best-fit alignment. The RMS between the retentive arm area of *Scan Data B* of each clasp specimen and that of its *Scan Data A*, denoted as RMS_{def} was calculated (Fig. 7).

2.8. Statistical analyses

As RMS_{acc} and RMS_{def} did not follow a normal distribution, a Box-Cox transformation was performed using a statistical analysis system (SAS 9.4, SAS Institute Inc, US). Two-way analyses of variance (ANOVA) with the transformed RMS_{acc} and RMS_{def} as the dependent variable, respectively, and the metal type and undercut engagement as classification variables were performed. The least-squares means for the different levels of the main effects were then compared. Repeated-measures ANOVA with f_0 , f_1 , f_2 , f_3 , f_4 , f_5 , f_6 , f_7 , f_8 , f_9 , and f_{10} as the dependent variables and the metal type and undercut engagement as the classification variables were performed. Within-subject and between-subject effects were also tested. The least-squares means of f_0 and f_{10} for different levels of the metal type and undercut engagement were

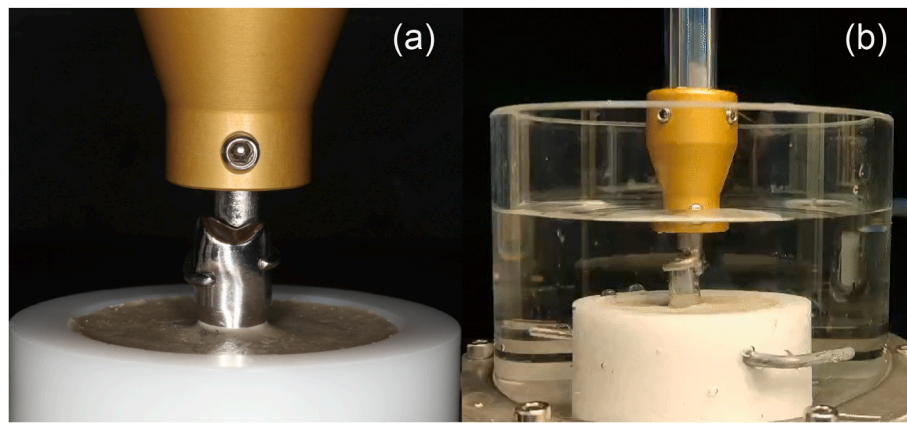


Fig. 6. Measurement of clasps' retentive force. (a) Fixation of clasp and die. (b) Insertion/removal cycle.

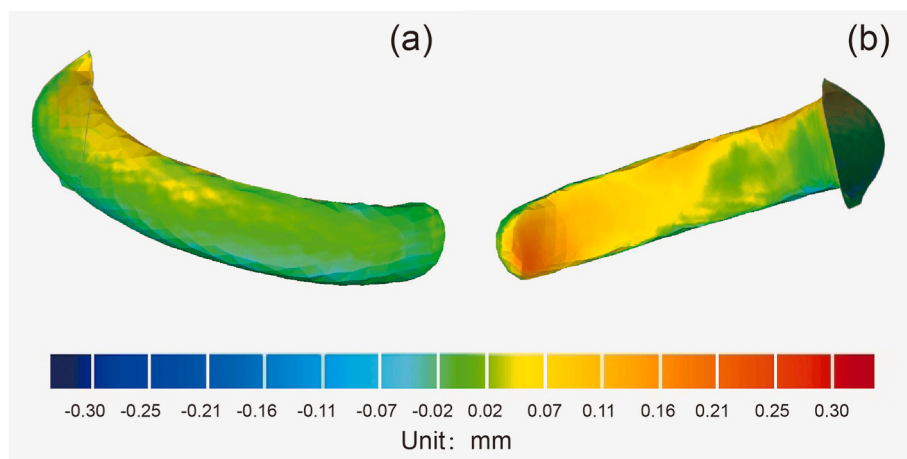


Fig. 7. Measurement of permanent deformation of retentive arms. (a) Polishing surface. (b) Intaglio surface.

compared. Similarly, one-way ANOVAs were performed with the transformed RMS_{acc} , f_0 , f_{10} , and RMS_{def} as the dependent variable, respectively, and the group as the classification variable. The mean values of each experimental group were compared with those of the control group using planned comparisons. All comparison results were plotted using the data analysis and graphing software program (OriginPro 2020b, OriginLab Corp, US).

3. Results

3.1. Accuracy of clasps and abutment dies

The RMSs between the tooth dies and their CAD data were $22.7 \pm 2.2 \mu\text{m}$. The RMS between the control group of clasps and their CAD data was $94.7 \pm 12.6 \mu\text{m}$. Mean RMSs between different experimental groups of clasps and their CAD data ranged from $51.5 \mu\text{m}$ to $79.9 \mu\text{m}$. Both the metal type and undercut engagement had significant effects on the accuracy of the SLM-built clasps ($P < .05$). No significant interaction effect between the metal type and undercut engagement was found on the accuracy of the SLM-built clasps ($P > .05$) (Table 4). For SLM-built clasps engaging the same undercuts, CP Ti and Ti-6Al-4V clasps showed higher accuracy than Co-Cr ones ($P < .05$), and no significant accuracy difference was found between CP Ti and Ti-6Al-4V clasps ($P > .05$) (Fig. 8a). For SLM-built clasps made of the same metal, the clasps engaging 0.01-in undercuts had significantly higher accuracy than those engaging 0.02-in undercuts ($P < .05$) (Fig. 8b). This was due to excessive grinding and polishing of the clasps engaging 0.02-in undercuts such that they were seated successfully on the tooth dies. All experimental

Table 4

Two-way analysis of variance for root mean square of clasp specimens. RMS_{acc} , Root mean square between clasp arms, rest, and proximal plate area of scan data of each clasp specimen before insertion/removal test and that of CAD data. λRMS_{acc} , Transformed RMS_{acc} after Box-Cox transformation. Met, Metal type. Und, Undercut engagement.

Dependent variable	Source	Df	F	P
λRMS_{acc}	Model	5	8.65	<.001*
	Met	2	15.82	<.001*
	Und	1	7.57	.010*
	Met* Und	2	2.02	.150

*Mean difference significant ($P < .05$).

groups showed significantly higher accuracy than the control group ($P < .05$), except for the SLM-built Co-Cr clasps engaging 0.02-in undercuts ($P > .05$). The accuracy of this group of clasps was similar to that of the control group (Fig. 9).

3.2. Fracture of clasps

After 7500 insertion/removal cycles, the retentive arm of one SLM-built Co-Cr clasp specimen engaging a 0.02-in undercut fractured at the clasp shoulder, while that of another fractured at the same site after 10,500 cycles. Fig. 10 shows the fracture surface of the retentive arm of the failed specimen. The crack originated from the side of the clasp shoulder away from the rest, where the maximum von Mises stress occurred [27]. Subsequently, the crack propagated to the middle and

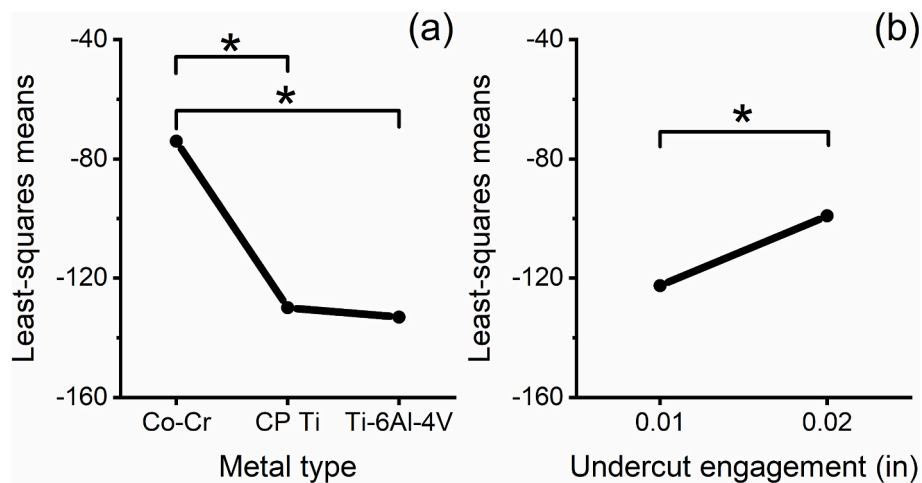


Fig. 8. Least-squares means of transformed RMS_{acc} for main effects. RMS_{acc}, Root mean square between clasp arms, rest, and proximal plate area of scan data of each clasp specimen before insertion/removal test and that of CAD data. (a) Metal type. (b) Undercut engagement. Co-Cr, Cobalt-chromium. CP Ti, Commercially pure titanium. Ti alloy, Ti-6Al-4V. *Mean difference significant ($P < .05$).

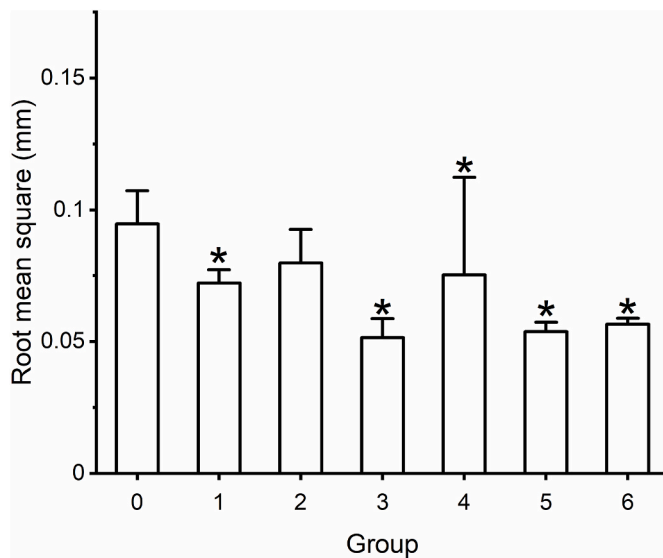


Fig. 9. RMS_{acc} of different groups of clasps. RMS_{acc}, Root mean square between clasp arms, rest, and proximal plate area of scan data of each clasp specimen before insertion/removal test and that of CAD data. Group 0, Control group, cast Co-Cr clasp specimens engaging 0.01-in undercuts. Group 1, SLM-built Co-Cr clasp specimens engaging 0.01-in undercuts. Group 2, SLM-built Co-Cr clasp specimens engaging 0.02-in undercuts. Group 3, SLM-built CP Ti clasp specimens engaging 0.01-in undercuts. Group 4, SLM-built CP Ti clasp specimens engaging 0.02-in undercuts. Group 5, SLM-built Ti-6Al-4V clasp specimens engaging 0.01-in undercuts. Group 6, SLM-built Ti-6Al-4V clasp specimens engaging 0.02-in undercuts. SLM, Selective laser melting. Co-Cr, Cobalt-chromium. CP Ti, Commercially pure titanium. Ti alloy, Ti-6Al-4V. *Mean significant difference between experimental and control group ($P < .05$).

eventually terminated on the side of the clasp shoulder near the rest. The fracture surface of the SLM-built clasps was uneven, and many dimples existed, which indicated that ductile fracture occurred on the SLM-built Co-Cr clasps. Two additional specimens were added to the experimental group of clasps to ensure that there were six specimens in each group.

3.3. Long-term retention of clasps

Fig. 11 shows the change in the retentive force of the clasps across different cycling sequences. Table 5 shows that the retentive force did

not change significantly across different cycling sequences ($P > .05$) and that the change in the retentive force of SLM-built clasps across different cycling sequences did not depend on the metal type and undercut engagement ($P > .05$) (Table 5). For SLM-built clasps engaging the same undercuts, the Co-Cr clasps had a significantly higher initial and final retentive force than CP Ti and Ti-6Al-4V ones ($P < .05$); and no significant difference in the initial or final retentive force was found between CP Ti and Ti-6Al-4V ones ($P > .05$) (Figs. 12a and 13a). This is owing to the higher elastic modulus of the Co-Cr alloy than that of CP Ti and Ti-6Al-4V alloy [8,19,27]. For SLM-built clasps made of the same metal, the clasps engaging 0.02-in undercuts had significantly higher initial and final retentive forces than those engaging 0.01-in undercuts ($P < .05$) (Figs. 12b and 13b). SLM-built CP Ti or Ti-6Al-4V clasps engaging 0.01-in undercuts had significantly lower initial and final retentive forces than the control group ($P < .05$); SLM-built CP Ti clasps engaging 0.02-in undercuts had the same initial retentive force ($P > .05$) but a lower final retentive force ($P < .05$) compared with that of the control group; while the other experimental groups of clasps had similar initial and final retentive forces as those of the control group ($P > .05$) (Fig. 14).

3.4. Permanent deformation of retentive arms

Both the metal type and undercut engagement had significant effects on the permanent deformation of the retentive arms of the SLM-built clasps ($P < .05$); no significant interaction effect was found between the metal type and undercut engagement ($P > .05$) (Table 6). For SLM-built clasps engaging the same undercuts, the permanent deformation of CP Ti clasps was significantly greater than that of Co-Cr and Ti-6Al-4V ones ($P < .05$). This was related to the lower yield strength of CP Ti compared to those of Co-Cr and Ti-6Al-4V alloys. No significant permanent deformation difference was found between the Co-Cr and Ti-6Al-4V clasps ($P > .05$) (Fig. 15a). For SLM-built clasps made of the same metal, the permanent deformation of clasps engaging 0.01-in undercuts was less than that of clasps engaging 0.02-in undercuts ($P < .05$) (Fig. 15b). The permanent deformation of the SLM-built Co-Cr and Ti-6Al-4V clasps engaging 0.01-in undercuts was less ($P < .05$) and that of SLM-built CP Ti clasps engaging 0.02-in undercuts was greater ($P < .05$) than that of the control group (Fig. 16).

4. Discussion

Tasaka et al. [33] showed that the deviation between cast Co-Cr clasps and the tooth die was -85.2 to 72.80 μm , and that between the

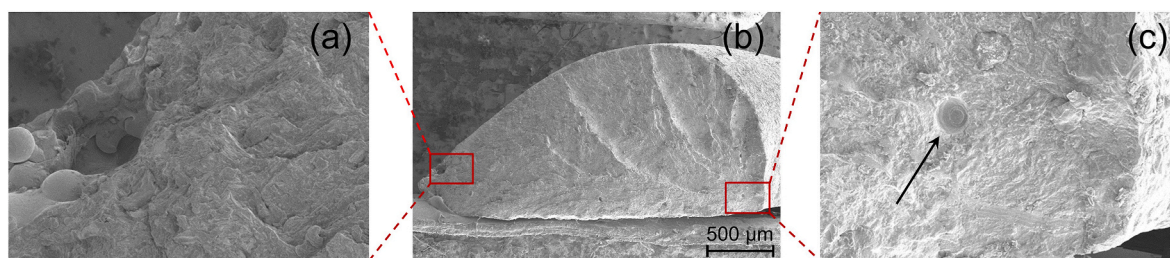


Fig. 10. Scanning electron microscope of fracture surface of retentive arms. (a) Crack initiation area of cobalt-chromium clasp. (b) Fracture surface. (c) Crack termination area; arrow indicates dimple.

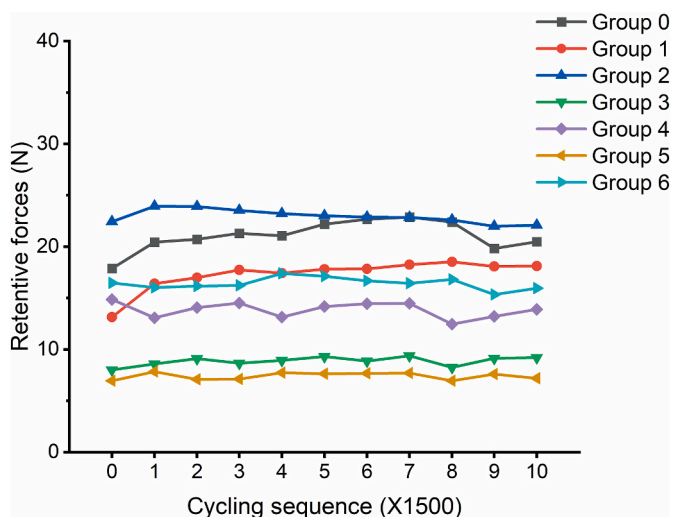


Fig. 11. Retentive force changes of clasps during cyclic insertion/removal. Group 0, Control group, cast Co–Cr clasp specimens engaging 0.01-in undercut. Group 1, SLM-built Co–Cr clasp specimens engaging 0.01-in undercuts. Group 2, SLM-built Co–Cr clasp specimens engaging 0.02-in undercuts. Group 3, SLM-built CP Ti clasp specimens engaging 0.01-in undercuts. Group 4, SLM-built CP Ti clasp specimens engaging 0.02-in undercuts. Group 5, SLM-built Ti–6Al–4V clasp specimens engaging 0.01-in undercuts. Group 6, SLM-built Ti–6Al–4V clasp specimens engaging 0.02-in undercuts. SLM, Selective laser melting. Co–Cr, Cobalt-chromium. CP Ti, Commercially pure titanium. Ti alloy, Ti–6Al–4V.

Table 5

Repeated-measures analysis of variance for within-subject and between-subject effects. Met, Metal type. Und, Undercut engagement. Cyc, Cycling sequence.

Classification variables	Source	Df	F	P
Met and Und	Cyc	10	1.65	.197
	Cyc*Met	20	1.37	.252
	Cyc*Und	10	2.38	.096
	Met	2	10.89	<.001*
	Und	1	14.52	.001*

*Mean difference significant ($P < .05$).

SLM-built Co–Cr clasps and tooth die was -3.20 to $52.40 \mu\text{m}$. Tan et al. [24] showed that the mean RMS values between the scan data of SLM-built Ti–6Al–4V clasps and their CAD data were $50.95 \pm 5.79 \mu\text{m}$. The accuracy of the clasps in these studies was similar to that in this study. Takahashi et al. [34] suggested that a gap of no more than $120 \mu\text{m}$ between the clasp and tooth would be acceptable for clinical use. Therefore, the accuracy of the clasp specimens in this study met the needs of dental clinics and could represent actual clinical situations.

The retentive force of the clasp was primarily derived from the friction between the clasp and tooth [26]. Reciprocating sliding wear tests [35] showed that the coefficient of friction (COF) between cast pure

Ti and human enamel was 0.1 before 100 cycles in the saliva condition. Similar tests [36] showed that the COF between cast pure Ti and human enamel was 0.13, and that between cast pure Ti and human enamel was 0.12 in the initial cycles. The COF between polished cast Co–Cr alloy and human enamel was 0.09, whereas the COF between sandblasted cast Co–Cr alloy and human enamel was 0.24 in the saliva condition in the study by Sato et al. [37]. The friction and wear between dental restorative materials and human enamel are complex processes. The COF is affected by many factors, such as hardness, surface roughness, and normal load. However, there is yet to be an accepted standard for this purpose. Moreover, there is a need for further research on the friction and wear between SLM-built metals and human enamel. During repeated insertion/removal, plastic deformation of the clasp arms and wear between the clasp and tooth die occur. Debris is generated between the clasp and tooth die, which increases the COF [35,36]. However, such rapid wear does not occur when a patient inserts an RPD and removes it from the mouth. Additionally, patients regularly clean RPDs. There was no accumulation of debris between the clasps and teeth. Consequently, the retentive force of the clasps after the patient wears the RPD for 10 years may be lower than the final retentive force of the clasps reported in this study. Before each measurement of the retentive forces, the debris between the clasp and tooth die should have been cleaned.

Unlike polymer clasps, which age in the mouth, thermocycling or simulating the oral temperature is not necessary for metal clasps. The test conditions were maintained at room temperature. Some researchers performed tests using artificial saliva or purified water to simulate the oral environment. In reciprocating sliding wear tests [35], the COF between cast CP Ti and living human teeth remained almost constant after 500 cycles under saliva or dry conditions. However, the COF increased more slowly in the first 500 cycles under saliva conditions. Therefore, this study was conducted using purified water.

The retentive force of the clasps changed with an increase in the number of insertion/removal cycles. The retention change of the clasps should also be emphasized to ensure that the RPD functions stably in the patient’s mouth for a long time. The retention changes of clasps in different material types of tooth dies may differ. In a study by Tanaka et al. [38], although there was no statistically significant difference between the initial retentive force of cast Co–Cr clasps on silver palladium copper alloy (Ag–Pd) full-metal crowns (FMC) and that of cast Co–Cr clasps on monolithic zirconia crowns (MZC), the retentive force of cast Co–Cr clasps on Ag–Pd FMC decreased significantly after 3000 insertion/removal cycles. In contrast, the retentive force of the cast Co–Cr clasps on the MZC was significantly reduced after 5000 insertion cycles of emplacement/dislocation. The materials used to make tooth dies include stainless steel, Co–Cr alloys, glass ceramics, and zirconia. Compared to zirconia, the wear resistance of glass ceramics is closer to that of enamel. In a study on the wear between dental restorative materials and natural teeth [39], the volume loss of teeth against leucite glass-ceramic was significantly greater than that of teeth against stainless steel. The wear resistance of metals is closely related to their hardness. Harder metals tend to exhibit better wear resistance. The Co–Cr alloy has a higher hardness, whereas 304 stainless steel has a hardness closer to that of human enamel. In this study, 304 stainless

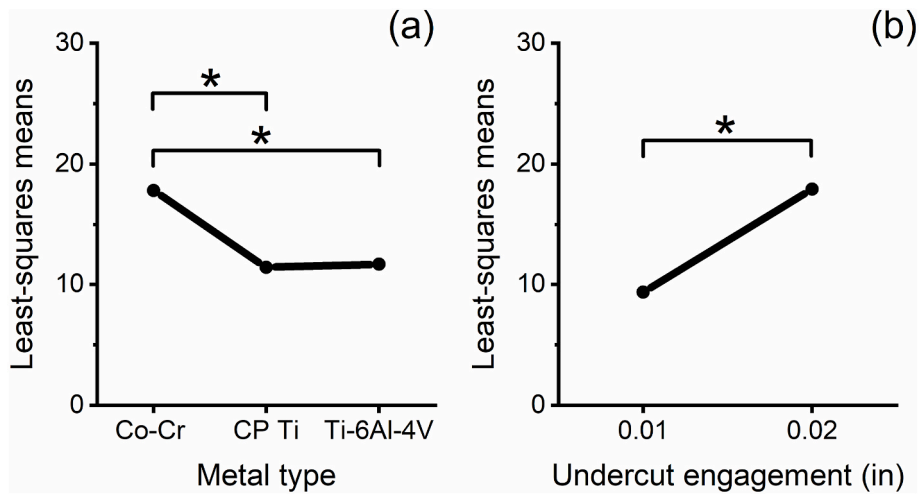


Fig. 12. Least-squares means of initial retentive force for main effects. (a) Metal type. (b) Undercut engagement. Co-Cr, Cobalt-chromium. CP Ti, Commercially pure titanium. Ti alloy, Ti-6Al-4V. *Mean difference significant ($P < .05$).

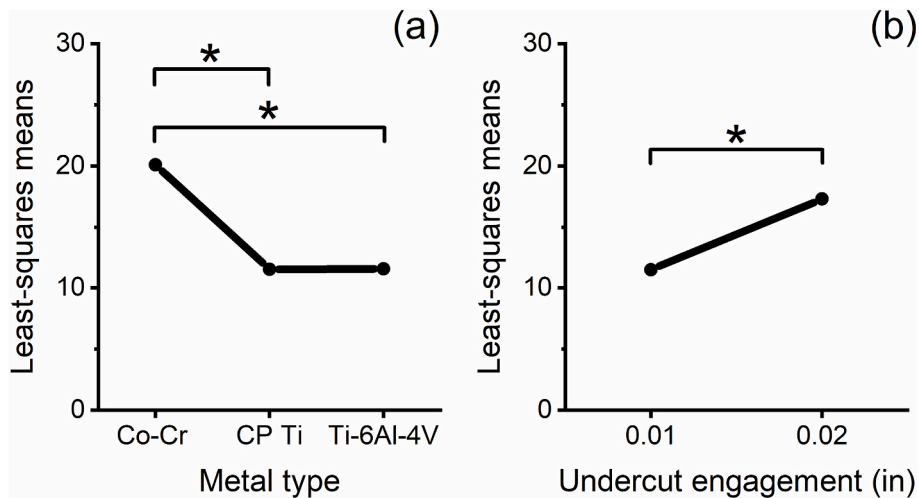


Fig. 13. Least-squares means of final retentive force for main effects. (a) Metal type. (b) Undercut engagement. Co-Cr, Cobalt-chromium. CP Ti, Commercially pure titanium. Ti alloy, Ti-6Al-4V. *Mean difference significant ($P < .05$).

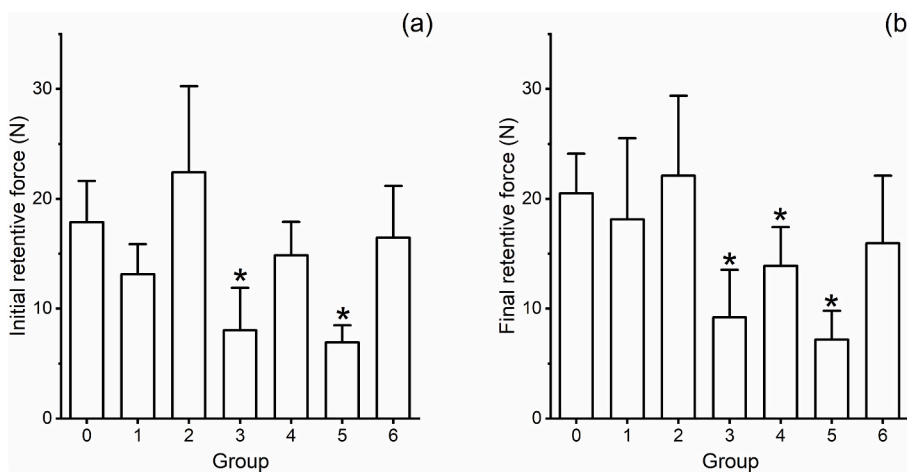


Fig. 14. Comparison of initial retentive force (a) and final retentive force (b). Group 0, Control group, cast Co-Cr clasp specimens engaging 0.01-in undercuts. Group 1, SLM-built Co-Cr clasp specimens engaging 0.01-in undercuts. Group 2, SLM-built Co-Cr clasp specimens engaging 0.02-in undercuts. Group 3, SLM-built CP Ti clasp specimens engaging 0.01-in undercuts. Group 4, SLM-built CP Ti clasp specimens engaging 0.02-in undercuts. Group 5, SLM-built Ti-6Al-4V clasp specimens engaging 0.01-in undercuts. Group 6, SLM-built Ti-6Al-4V clasp specimens engaging 0.02-in undercuts. SLM, Selective laser melting. Co-Cr, Cobalt-chromium. CP Ti, Commercially pure titanium. Ti alloy, Ti-6Al-4V. *Mean significant difference from control group ($P < .05$).

Table 6

Two-way analysis of variance for permanent deformation of retentive arms. RMS_{def} , Root mean square between retentive arm area of scan data of each specimen before insertion/removal test and that of its scan data after insertion/removal test. λ_1RMS_{def} , Transformed RMS_{def} after Box-Cox transformation. Met, Metal type. Und, Undercut engagement.

Dependent variable	Source	Df	F	P
λ_1RMS_{def}	Model	5	15.34	<.001*
	Met	2	15.40	<.001*
	Und	1	45.00	<.001*
	Met*Und	2	0.44	.651

*Mean difference significant ($P < .05$).

steel was used to manufacture the tooth dies.

It was found that the measured initial retentive force of the SLM-built Co–Cr clasps engaging 0.02-in undercuts was slightly lower than we estimated. This may be due to the excessive grinding and polishing of this group of clasps to ensure that they could be seated smoothly on tooth dies. This was also indicated by the slightly lower accuracy of this group of clasps compared with the other groups of SLM-built clasps. The overall results showed that the initial retentive force of SLM-built Co–Cr clasps engaging 0.01-in undercuts and CP Ti and Ti–6Al–4V clasps engaging 0.02-in undercuts was comparable to that of the control group. Compared with the control group, SLM-built Co–Cr clasps engaging 0.01-in undercuts and Ti–6Al–4V clasps engaging 0.02-in undercuts had a similar final retentive force and less permanent deformation; SLM-built CP Ti clasps engaging 0.02-in undercuts had less final retentive forces and greater permanent deformation. Previous researchers [17,20] showed that when the vertical deflection was 0.01 inches, the initial bending load for SLM-built Co–Cr clasp arms was significantly lower than that for cast Co–Cr clasp groups. In contrast, the initial retentive force of the SLM-built Co–Cr clasps engaging 0.01-in undercuts in this experiment was equal to that of the control group. The fatigue life of SLM-built CP clasp arms was 9327 ± 1159 when the vertical deflection at the tip was 0.02 inches in the experiment of Yu et al. [40], while none of the SLM-built CP Ti clasps engaging 0.02-in undercuts fractured after 15,000 cycles of insertion/removal in this experiment. Tan et al. [24] showed that all specimens of SLM-built Ti–6Al–4V clasps engaging 0.03-in undercuts fractured after 4000 cycles of insertion/removal. In contrast, SLM-built Ti–6Al–4V clasps engaging 0.02-in undercuts did not fracture after 15,000 insertion/removal cycles, and their long-term retention and permanent deformation of the retentive arms were comparable to those of the control group.

The limitations of this study are as follows. First, the effects of both the angle of cervical convergence and depth of the undercut on the retention of clasps should be explored. However, only the undercut depth was considered in this study. Second, it was assumed that the clasps did not rotate during insertion and removal. However, it is difficult to ensure that the retentive and reciprocal arms are not in contact with the abutment tooth simultaneously, resulting in an unbalanced force being applied to the crown of the abutment tooth in the buccolingual direction. Moreover, the physiological mobility of the periodontal ligament also helps the clasp rotate during insertion or dislocation from the abutment tooth. Moreover, clasps are not always dislodged along the insertion path during the removal of the RPD from the patient’s mouth.

Traditionally, prefabricated clasp wax patterns have been used to fabricate various types of clasps, including circumferential, I bars, and ring clasps. The size of the clasp arm is limited by the wax pattern used. The application of CAD/CAM in dentistry makes it possible to change the size of the clasp arm, including the width and thickness of the profile and taper from the tip to the body of the clasp arm. However, the size of the clasp arm differs among studies. Considering that 3Shape CAD software is widely used by many dental hospitals and laboratories worldwide, the default size of the clasp arm provided by CAD software was adopted in this experiment. In future research, the structural parameters of the clasp arm will be optimized. Optimal parameters can be further explored according to the methods used in this study. It is also necessary to optimize the structural parameters of other RPD components, such as the lingual bar. Furthermore, the application of cellular structures in RPDs, which are designed by constructive generative design [41] and built with high-strength amorphous alloys [42], helps to cushion the occlusal surface of artificial teeth from excessive bite force and controls the stress and displacement of RPDs to protect the mucosa and bone tissues under RPDs.

SLM-built RPD frameworks require sandblasting and polishing because of their relatively high surface roughness. Hybrid additive and subtractive manufacturing have been introduced in dentistry to solve these problems. For example, some scholars have attempted to manufacture Co–Cr clasps via repeated laser sintering and milling [43,44]. After several layers were built by laser sintering, high-speed milling of the contours to a fine finish was performed. The sintering and milling were repeated until a part was constructed. The Co–Cr clasps built in this way had a smoother surface and better fit. There have been no reports of RPD frameworks manufactured using this technology. However, this technology is becoming increasingly popular in dentistry.

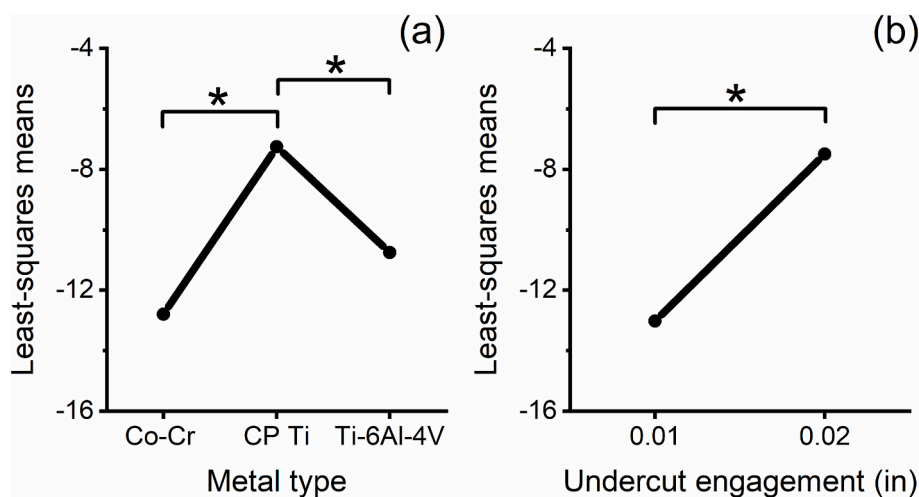


Fig. 15. Least-squares means of transformed RMS_{def} for main effects. RMS_{def} , Root mean square between retentive arm area of scan data of each specimen before insertion/removal test and that of its scan data after insertion/removal test. (a) Metal type. (b) Undercut engagement. Co–Cr, Cobalt-chromium. CP Ti, Commercially pure titanium. Ti alloy, Ti–6Al–4V. *Mean difference significant ($P < .05$).

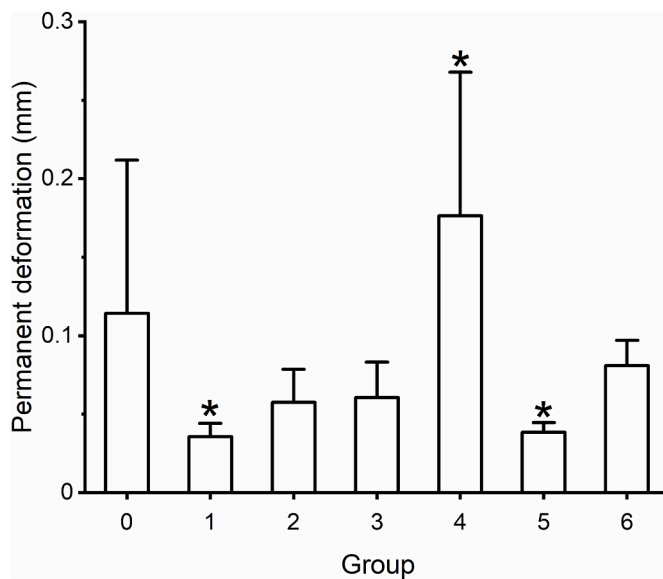


Fig. 16. Permanent deformation of retentive arms. Group 0, Control group, cast Co–Cr clasp specimens engaging 0.01-in undercuts. Group 1, SLM-built Co–Cr clasp specimens engaging 0.01-in undercuts. Group 2, SLM-built Co–Cr clasp specimens engaging 0.02-in undercuts. Group 3, SLM-built CP Ti clasp specimens engaging 0.01-in undercuts. Group 4, SLM-built CP Ti clasp specimens engaging 0.02-in undercuts. Group 5, SLM-built Ti–6Al–4V clasp specimens engaging 0.01-in undercuts. Group 6, SLM-built Ti–6Al–4V clasp specimens engaging 0.02-in undercuts. SLM, Selective laser melting. Co–Cr, Cobalt-chromium. CP Ti, Commercially pure titanium. Ti alloy, Ti–6Al–4V. *Mean significant difference from control group ($P < .05$).

5. Conclusions

Within the limitations of this in vitro study, the following conclusions were drawn:

1. The accuracy of the SLM-built Co–Cr, CP Ti, and Ti–6Al–4V clasps was better than that of cast Co–Cr clasps fabricated by 3D-printed resin casting.
2. SLM-built Co–Cr clasps engaging 0.01-in undercuts and CP Ti and Ti–6Al–4V clasps engaging 0.02-in undercuts had similar initial retentive forces as cast Co–Cr clasps engaging 0.01-in undercuts.
3. SLM-built Co–Cr clasps engaging 0.01-in undercuts and Ti–6Al–4V clasps engaging 0.02-in undercuts had similar final retentive forces as cast Co–Cr clasps engaging 0.01-in undercuts and lower permanent deformation than cast Co–Cr clasps engaging 0.01-in undercuts. SLM-built CP Ti clasps engaging 0.02-in undercuts had lower final retentive forces and higher permanent deformation than cast Co–Cr clasps engaging 0.01-in undercuts.
4. Considering the long-term retention and permanent deformation of the retentive arms, Co–Cr and Ti–6Al–4V alloys, except CP Ti, are recommended for printing denture clasps. SLM-built Co–Cr clasps should engage 0.01-in undercuts, and Ti–6Al–4V clasps should engage 0.02-in undercuts.

Credit authorship contribution statement

Kenan Ma: Methodology, Formal analysis, Investigation, Writing - Original Draft, Visualization. **Hu Chen:** Methodology, Writing - Reviewing & Editing, Supervision, Funding acquisition. **Yanru Shen:** Formal analysis, Investigation, Writing - Reviewing & Editing. **Yuqing Guo:** Formal analysis, Investigation, Writing - Reviewing & Editing. **Weiwei Li:** Methodology, Formal analysis, Writing - Reviewing & Editing. **Yong Wang:** Writing - Reviewing and Editing, Supervision. **Yicha Zhang:** Conceptualization, Methodology, Writing - Review & Editing,

Supervision, Project administration. **Yuchun Sun:** Conceptualization, Methodology, Writing - Review & Editing, Supervision, Project administration, Funding acquisition.

Declaration of competing interest

None Declared.

Acknowledgments

This work was supported by the State Key R&D Program of China (Grant No. 2019YFB1706900) and Capital's Funds for Health Improvement and Research (Grant No. 2022-2Z-4106).

References

- [1] World Health Organization, Ageing and health. <https://www.who.int/news-room/fact-sheets/detail/ageing-and-health>, 2022. (Accessed 5 January 2023).
- [2] Chinese Stomatological Association, *The 4th National Oral Health Survey Report*, People's Medical Publishing House Co. Ltd, Beijing, 2018.
- [3] A.R. Jordan, H. Stark, I. Nitschke, W. Micheelis, F. Schwendicke, Epidemiological trends, predictive factors, and projection of tooth loss in Germany 1997–2030: part I. missing teeth in adults and seniors, *Clin. Oral Invest.* 25 (1) (2010) 67–76, <https://doi.org/10.1007/s00784-020-03266-9>.
- [4] M.A. Peres, R. Lalloo, Tooth loss, denture wearing and implants: findings from the national study of adult oral health 2017–18, *Aust. Dent. J.* 65 (S1) (2020) S23–S31, <https://doi.org/10.1111/adj.12761>.
- [5] Centers for Disease Control and Prevention, Oral health surveillance report: trends in dental caries and sealants, tooth retention, and edentulism, United States, 1999–2004 to 2011–2016. <https://www.cdc.gov/oralhealth/publications/OHSR-2019-index.html#print>, 2019. (Accessed 5 January 2023).
- [6] H. Nishiyama, A. Taniguchi, S. Tanaka, K. Baba, Novel fully digital workflow for removable partial denture fabrication, *J. Prosthodont. Res.* 64 (1) (2020) 98–103, <https://doi.org/10.1016/j.jpor.2019.05.002>.
- [7] Y. Zhang, K. Li, H. Yu, J. Wu, B. Gao, Digital fabrication of removable partial dentures made of titanium alloy and zirconium silicate micro-ceramic using a combination of additive and subtractive manufacturing technologies, *Rapid Prototyp. J.* 27 (1) (2021) 93–98, <https://doi.org/10.1108/RPJ-02-2020-0040>.
- [8] M. Revilla-León, M. Özcan, Additive manufacturing technologies used for 3D metal printing in dentistry, *Curr. Oral. Health. Rep.* 4 (3) (2017) 201–208, <https://doi.org/10.1007/s40496-017-0152-0>.
- [9] B. Vandenbroucke, J.P. Kruth, Selective laser melting of biocompatible metals for rapid manufacturing of medical parts, *Rapid Prototyp. J.* 13 (4) (2007) 196–203, <https://doi.org/10.1108/13552540710776142>.
- [10] L. Wu, H. Zhu, X. Gai, Y. Wang, Evaluation of the mechanical properties and porcelain bond strength of cobalt-chromium dental alloy fabricated by selective laser melting, *J. Prosthet. Dent* 111 (1) (2014) 51–55, <https://doi.org/10.1016/j.prosdent.2013.09.011>.
- [11] L. Tonelli, A. Fortunato, L. Ceschini, CoCr alloy processed by selective laser melting (SLM): effect of laser energy density on microstructure, surface morphology, and hardness, *J. Manuf. Process.* 52 (2020) 106–119, <https://doi.org/10.1016/j.jmapro.2020.01.052>.
- [12] H. Chen, H. Li, Y. Zhao, X. Zhang, Y. Wang, P. Lyu, Adaptation of removable partial denture frameworks fabricated by selective laser melting, *J. Prosthet. Dent* 122 (3) (2019) 316–324, <https://doi.org/10.1016/j.prosdent.2018.11.010>.
- [13] P. Soltanzadeh, M.S. Suprono, M.T. Kattadiyil, C. Goodacre, W. Gregorius, An in vitro investigation of accuracy and fit of conventional and CAD/CAM removable partial denture frameworks, *J. Prosthodont.* 28 (5) (2019) 547–555, <https://doi.org/10.1111/jopr.12997>.
- [14] A. Tasaka, T. Shimizu, Y. Kato, H. Okano, Y. Ida, S. Higuchi, S. Yamashita, Accuracy of removable partial denture framework fabricated by casting with a 3D printed pattern and selective laser sintering, *J. Prosthodont. Res.* 64 (2) (2020) 224–230, <https://doi.org/10.1016/j.jpor.2019.07.009>.
- [15] S. Hwang, S. An, U. Robles, R.C. Rumpf, Process parameter optimization for removable partial denture frameworks manufactured by selective laser melting, *J. Prosthet. Dent* (2021), <https://doi.org/10.1016/j.prosdent.2021.04.021>.
- [16] S. Yager, J. Ma, H. Özcan, H.I. Kilinc, A.H. Elwany, I. Karaman, Mechanical properties and microstructure of removable partial denture clasps manufactured using selective laser melting, *Addit. Manuf.* 8 (2015) 117–123, <https://doi.org/10.1016/j.addma.2015.09.005>.
- [17] S.Y. Kim, S.-Y. Shin, J.H. Lee, Effect of cyclic bend loading on a cobalt-chromium clasp fabricated by direct metal laser sintering, *J. Prosthet. Dent* 119 (6) (2018) 1027.e1021–1027.e1027, <https://doi.org/10.1016/j.prosdent.2018.03.016>.
- [18] M. Mutschler, F. Schweitzer, S. Spintzyk, J. Geis-Gerstorfer, F. Huettig, Retention forces of prosthetic clasps over a simulated wearing period of six years in-vitro: direct metal laser melting versus dental casting, *Materials* 13 (23) (2020) 5339, <https://doi.org/10.3390/ma13235339>.
- [19] W. Xie, M. Zheng, J. Wang, X. Li, The effect of build orientation on the microstructure and properties of selective laser melting Ti-6Al-4V for removable partial denture clasps, *J. Prosthet. Dent* 123 (1) (2020) 163–172, <https://doi.org/10.1016/j.prosdent.2018.12.007>.

- [20] Y. Kajima, A. Takaichi, T. Nakamoto, T. Kimura, Y. Yogo, M. Ashida, H. Doi, N. Nomura, H. Takahashi, T. Hanawa, Fatigue strength of Co-Cr-Mo alloy clasps prepared by selective laser melting, *J. Mech. Behav. Biomed. Mater.* 59 (2016) 446–458, <https://doi.org/10.1016/j.jmbbm.2016.02.032>.
- [21] R. Kaiser, K. Williamson, C. O'Brien, S. Ramirez-Garcia, D.J. Browne, The influence of cooling conditions on grain size, secondary phase precipitates and mechanical properties of biomedical alloy specimens produced by investment casting, *J. Mech. Behav. Biomed. Mater.* 24 (2013) 53–63, <https://doi.org/10.1016/j.jmbbm.2013.04.013>.
- [22] S. Wen, S. Li, Q. Wei, C. Yan, S. Zhang, Y. Shi, Effect of molten pool boundaries on the mechanical properties of selective laser melting parts, *J. Mater. Process. Technol.* 214 (11) (2014) 2660–2667, <https://doi.org/10.1016/j.jmatprotec.2014.06.002>.
- [23] Y. Kajima, A. Takaichi, T. Nakamoto, T. Kimura, N. Kittikundecha, Y. Tsutsumi, N. Nomura, A. Kawasaki, H. Takahashi, T. Hanawa, N. Wakabayashi, Effect of adding support structures for overhanging part on fatigue strength in selective laser melting, *J. Mech. Behav. Biomed. Mater.* 78 (2018) 1–9, <https://doi.org/10.1016/j.jmbbm.2017.11.009>.
- [24] F. Tan, J. Song, C. Wang, Y. Fan, H. Dai, Titanium clasp fabricated by selective laser melting, CNC milling, and conventional casting: a comparative in vitro study, *J. Prosthodont. Res.* 63 (1) (2019) 58–65, <https://doi.org/10.1016/j.jpor.2018.08.002>.
- [25] A.B. Carr, D.T. Brown, in: *McCracken's Removable Partial Prosthodontics, thirteenth ed., Elsevier Mosby, St. Louis, Mo, 2016*.
- [26] A.A. Alsheghri, O. Alageel, E. Caron, O. Ciobanu, F. Tamimi, J. Song, An analytical model to design circumferential clasps for laser-sintered removable partial dentures, *Dent. Mater.* 34 (10) (2018) 1474–1482, <https://doi.org/10.1016/j.dental.2018.06.011>.
- [27] K. Ma, H. Chen, Y. Shen, Y. Zhou, Y. Wang, Y. Sun, Finite element analyses of retention of removable partial denture circumferential clasps manufactured by selective laser melting, *J. Peking Univ. (Heal. Sci.)* 54 (1) (2022) 105–112, <https://doi.org/10.19723/j.issn.1671-167X.2022.01.017>.
- [28] A. Kudzal, B. McWilliams, C. Hofmeister, F. Kellogg, J. Yu, J. Taggart-Scarff, J. Liang, Effect of scan pattern on the microstructure and mechanical properties of powder bed fusion additive manufactured 17-4 stainless steel, *Mater. Des.* 133 (2017) 205–215, <https://doi.org/10.1016/j.matdes.2017.07.047>.
- [29] N. Nadammal, T. Mishurova, T. Fritsch, I. Serrano-Munoz, A. Kromm, C. Haberland, P.D. Portella, G. Bruno, Critical role of scan strategies on the development of microstructure, texture, and residual stresses during laser powder bed fusion additive manufacturing, *Addit. Manuf.* 38 (2021), 101792, <https://doi.org/10.1016/j.addma.2020.101792>.
- [30] A. Simchi, Direct laser sintering of metal powders: mechanism, kinetics and microstructural features, *Mater. Sci. Eng. A-Struct. Mater. Prop. Microstruct. Process.* 428 (1) (2006) 148–158, <https://doi.org/10.1016/j.msea.2006.04.117>.
- [31] D. Gu, Y.-C. Hagedorn, W. Meiners, G. Meng, R.J.S. Batista, K. Wissenbach, R. Poprawe, Densification behavior, microstructure evolution, and wear performance of selective laser melting processed commercially pure titanium, *Acta Mater.* 60 (9) (2012) 3849–3860, <https://doi.org/10.1016/j.actamat.2012.04.006>.
- [32] S. Hwang, S. An, U. Robles, R.C. Rumpf, Process parameter optimization for removable partial denture frameworks manufactured by selective laser melting, *J. Prosthet. Dent.* (2021), <https://doi.org/10.1016/j.prosdent.2021.04.021>.
- [33] A. Tasaka, Y. Kato, K. Odaka, S. Matsunaga, T. Goto, S. Abe, S. Yamashita, Accuracy of clasps fabricated with three different CAD/CAM technologies: casting, milling, and selective laser sintering, *Int. J. Prosthodont. (IJP)* 32 (6) (2019) 526–529, <https://doi.org/10.11607/ijp.6363>.
- [34] K. Takahashi, M. Torii, T. Nakata, N. Kawamura, H. Shimpo, C. Ohkubo, Fitness accuracy and retentive forces of additive manufactured titanium clasp, *J. Prosthodont. Res.* 64 (4) (2020) 468–477, <https://doi.org/10.1016/j.jpor.2020.01.001>.
- [35] H. Li, Z. Zhou, Wear behaviour of human teeth in dry and artificial saliva conditions, *Wear* 249 (10–11) (2001) 980–984, [https://doi.org/10.1016/S0043-1648\(01\)00835-3](https://doi.org/10.1016/S0043-1648(01)00835-3).
- [36] J. Zheng, X. Shi, Z. Zhou, Study on tribological behavior of human enamel sliding against various counterparts under Lubrication of artificial saliva, *Tribology* 24 (2) (2004) 139–143, <https://doi.org/10.3321/j.issn:1004-0595.2004.02.010>.
- [37] Y. Sato, Y. Abe, Y. Yuasa, Y. Akagawa, Effect of friction coefficient on Akers clasp retention, *J. Prosthet. Dent* 78 (1) (1997) 22–27, [https://doi.org/10.1016/s0022-3913\(97\)70083-0](https://doi.org/10.1016/s0022-3913(97)70083-0).
- [38] A. Tanaka, N. Miyake, H. Hotta, S. Takemoto, M. Yoshinari, S. Yamashita, Change in the retentive force of Akers clasp for zirconia crown by repetitive insertion and removal test, *J. Prosthodont. Res.* 63 (4) (2019) 447–452, <https://doi.org/10.1016/j.jpor.2019.02.005>.
- [39] J.W. Choi, I.H. Bae, T.H. Noh, S.W. Ju, T.K. Lee, J.S. Ahn, T.S. Jeong, J.B. Huh, Wear of primary teeth caused by opposed all-ceramic or stainless steel crowns, *J. Adv. Prosthodont.* 8 (1) (2016) 43–52, <https://doi.org/10.4047/jap.2016.8.1.43>.
- [40] H. Yu, K. Wen, Y. Liu, W. Wang, R. Ma, C. Qin, B. Gao, Fatigue resistance of pure titanium clasps prepared via selective laser melting, *J. Pract. Stomatol.* 34 (3) (2018) 323–326, <https://doi.org/10.3969/j.issn.1001-3733.2018.03.007>.
- [41] T. Vaneker, A. Bernard, G. Moroni, I. Gibson, Y. Zhang, Design for additive manufacturing: framework and methodology, *CIRP Ann.-Manuf. Technol.* 69 (2) (2020) 578–599, <https://doi.org/10.1016/j.cirp.2020.05.006>.
- [42] H. Li, Y. Zheng, Recent advances in bulk metallic glasses for biomedical applications, *Acta Biomater.* 36 (2016) 1–20, <https://doi.org/10.1016/j.actbio.2016.03.047>.
- [43] T. Nakata, H. Shimpo, C. Ohkubo, Clasp fabrication using one-process molding by repeated laser sintering and high-speed milling, *J. Prosthodont. Res.* 61 (3) (2017) 276–282, <https://doi.org/10.1016/j.jpor.2016.10.002>.
- [44] M. Torii, T. Nakata, K. Takahashi, N. Kawamura, H. Shimpo, C. Ohkubo, Fitness and retentive force of cobalt-chromium alloy clasps fabricated with repeated laser sintering and milling, *J. Prosthodont. Res.* 62 (3) (2018) 342–346, <https://doi.org/10.1016/j.jpor.2018.01.001>.